

Calorimetric study of nematic to smectic-*A* tricritical behavior

K. J. Stine and C. W. Garland

Department of Chemistry and Center for Material Science and Engineering, Massachusetts Institute of Technology, Cambridge, Massachusetts 02139

(Received 12 September 1988)

High-resolution heat capacity measurements have been made on six mixtures of 40.8 and 60.8, the butyl and hexyl homologs of alkoxybenzylidene octylaniline. The nematic (*N*)-smectic-*A* (*Sm-A*) transition becomes tricritical close to $X=0.35$, where X is the mole fraction of 60.8. The C_p data for a mixture with $X=0.35$ are well described by the tricritical exponent $\alpha=0.5$ and an amplitude ratio $A^-/A^+=1.6$, which is not a universal quantity for tricritical measurements over the accessible range of reduced temperatures. The small value of A^-/A^+ means that *N-Sm-A* tricriticality is further from classical Landau tricritical behavior than is the $^3\text{He-}^4\text{He}$ system. Analysis of C_p data over an extended range shows the importance of several correction terms to the leading singularity. In particular, there seems to be a small step discontinuity at T_c , which does not violate scaling at a tricritical point as it would for a second-order critical point.

I. INTRODUCTION

The nematic (*N*) to smectic-*A* (*Sm-A*) transition involves the development of a one-dimensional density modulation in an orientationally ordered fluid of long organic molecules. The study of critical behavior at the *N-Sm-A* transition is an active area of research.¹ It has been found experimentally that the effective critical exponents vary systematically with the temperature range of the nematic phase.^{2,3} The exponent α characterizing the critical heat capacity varies from values close to the theoretical 3D-XY value⁴ of -0.007 in two cases where the nematic range is wide,^{2,5} through intermediate positive values,⁶⁻⁸ to values close to $+0.50$ at tricritical points that have been observed in five cases.^{3,9-12} For sufficiently narrow nematic ranges, the *N-Sm-A* transition is first order.^{3,9} Each investigated system (pure compounds and mixtures) is well described by a single effective α value over a wide range of reduced temperature, and it is not clear whether the expected tricritical-to-XY crossover¹³ is too broad to be observed or whether the measured exponents are asymptotic values.

Hexyloxybenzylidene octylaniline (60.8) has a nematic range $\Delta T_N = T_{NI} - T_{NA}$ of 0.9 K and exhibits a strongly first order *N-Sm-A* transition.¹⁴ Butyloxybenzylidene octylaniline (40.8) has a nematic range of 14.7 K and exhibits a second-order *N-Sm-A* transition with $\alpha=0.15\pm 0.05$.⁷ We have carried out high-resolution ac calorimetric studies of the temperature variation of the heat capacity associated with the *N-Sm-A* transition in mixtures of 40.8 and 60.8. Such $C_p(T)$ data have been obtained for six samples with mole fractions $X_{60.8}$ between 0.10 and 0.50. We report the results of an extensive analysis with emphasis on the sample having $X_{60.8}=0.35$, which is close to the tricritical composition. A steplike correction term seems necessary for a good representation of the tricritical excess heat capacity ΔC_p , and its possible theoretical justification is discussed. Additional higher-order terms needed to improve the residu-

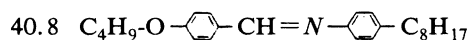
al pattern for the tricritical data over a wide range of reduced temperatures have also been considered. The apparent nonuniversality of the amplitude ratio A^-/A^+ for ΔC_p at tricritical points is discussed. We have also attempted to fit the tricritical ΔC_p data using two predicted forms for logarithmic corrections,^{15,16} and there is no strong evidence for such corrections over the presently accessible range of reduced temperatures.

II. METHOD AND RESULTS

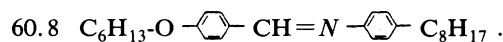
The ac calorimeter used in this work is a microcomputer-controlled instrument described in detail elsewhere.¹⁷ The specific heat C_p is the heat capacity per gram determined from

$$C_p = \frac{C_p(\text{obs}) - C_p(\text{empty})}{m}, \quad (1)$$

where $C_p(\text{obs})$ is the total observed heat capacity of the sample cell plus the liquid crystal, $C_p(\text{empty})$ is the heat capacity of the empty cell, and m is the mass of the liquid crystal sample in grams. The structural formulas of 40.8 and 60.8 are



and



The phase diagram presented in Fig. 1 includes temperatures for the *N-Sm-A* and *N-I* transitions obtained from the ac calorimetric data and also from a differential scanning calorimetry (DSC) study. Both ac calorimetry and DSC were used to study samples with $X_{60.8}=0.10, 0.20, 0.30, 0.35, 0.40,$ and 0.50 ; DSC measurements were also made on samples with $X_{60.8}=0.65, 0.83, 0.89,$ and 0.95 . The variation of C_p through the *N-Sm-A* and *N-I* transition regions in pure 40.8 is shown in Fig. 2. In this

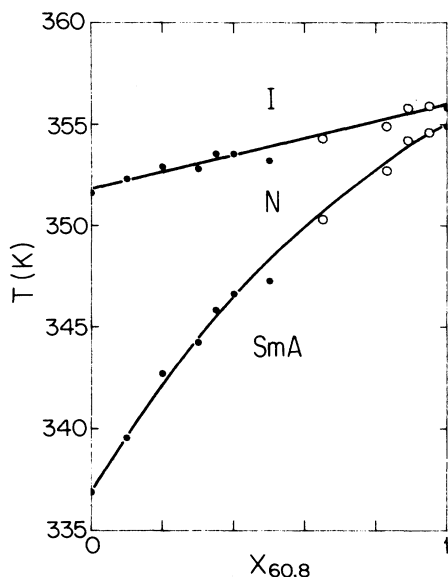


FIG. 1. Phase diagram for 40.8+60.8 mixtures. Transition temperatures were determined from ac calorimetry (●) and DSC (○).

case, the nematic range is 14.72 K (often expressed as the McMillan ratio $M \equiv T_{NA}/T_{NI} = 0.958$), and the N - $Sm-A$ peak is well removed from the N - I peak. The dashed curve in Fig. 2 represents the background chosen for the determination of the excess specific heat associated with the N - $Sm-A$ transition. This background curve, which will be denoted as $C_p(N-I)$, represents the specific-heat variation to be expected if only the N - I transition occurred. The N - I transitions were all weakly first order

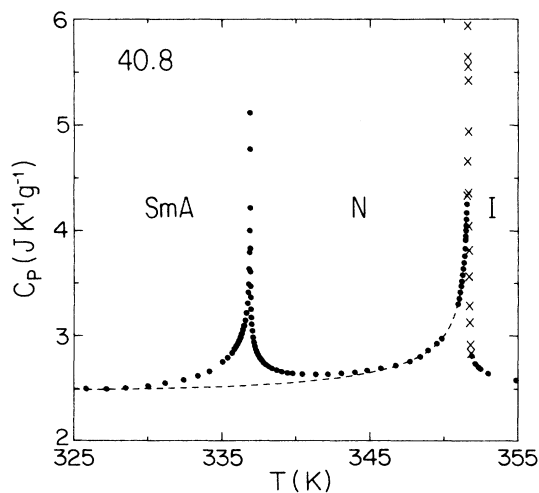


FIG. 2. Specific heat of 40.8. The dashed curve represents $C_p(N-I)$, the background curve used in Eq. (2) to determine the excess heat capacity associated with the N - $Sm-A$ transition. The points marked with a cross at the top of the N - I peak are apparent C_p values obtained in a two-phase coexistence region.

with coexistence regions 0.1–0.2 K wide. The variation of C_p through the N - $Sm-A$ and N - I transitions in pure 60.8 is shown in Fig. 3. In this case, the nematic range is only 0.87 K ($M=0.998$), and the N - $Sm-A$ transition is strongly first order with a coexistence region of 0.11 K. The variation of C_p through the N - $Sm-A$ and N - I transitions is shown in Fig. 4 for the $X_{60.8}=0.35$ sample, which we believe to be closest to the tricritical composition. For each sample, the curve $C_p(N-I)$ was subtracted from C_p and the resulting excess specific heat converted to dimensionless units via

$$\frac{\Delta C_p}{R} = [C_p - C_p(N-I)]\bar{M}/R, \quad (2)$$

where

$$\bar{M} = X_{40.8}M_{40.8} + X_{60.8}M_{60.8}, \quad (3)$$

$X_{40.8}$ and $X_{60.8}$ are the respective mole fractions, $M_{40.8} = 365.56 \text{ g mol}^{-1}$ and $M_{60.8} = 393.61 \text{ g mol}^{-1}$ are the respective molecular weights, and $R = 8.314 \text{ J K}^{-1} \text{ mol}^{-1}$ is the gas constant. \bar{M} is thus the effective molecular weight of the mixture. The temperature variation of $\Delta C_p/R$ is shown in Fig. 5 for all the investigated samples except pure 60.8. These excess heat capacity values were used in the analysis of the N - $Sm-A$ critical and tricritical behavior presented in Sec. III.

The N - $Sm-A$ transitions were all studied on a cooling run followed by a heating run. Over a period of ~ 100 h, we have observed an average drift rate dT_c/dt for these samples of -0.13 mK h^{-1} , which is very small compared to those reported in many other systems. Figure 6 shows a comparison of the heating and cooling data over the range $|T - T_{\text{peak}}| \leq 0.1 \text{ K}$ for the samples with $X_{60.8} = 0.30, 0.35,$ and 0.40 . Data points close to T_c that lie between the short vertical lines were omitted from the

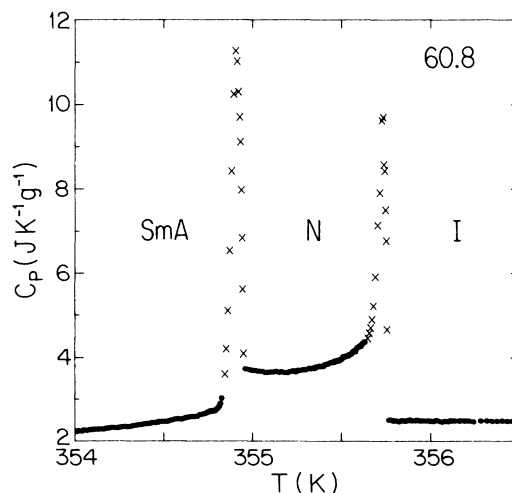


FIG. 3. Specific heat of 60.8. Both the N - I and N - $Sm-A$ transitions are strongly first order. Points indicated by a cross (×) are anomalous values obtained in two-phase coexistence regions.

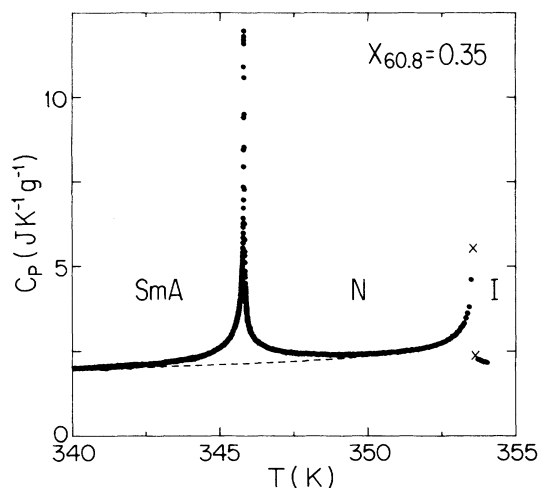


FIG. 4. Specific heat of the tricritical 40.8+60.8 mixture with mole fraction $X_{60.8}=0.35$. The dashed curve represents $C_p(N-I)$ as described in the text and in the legend of Fig. 2. Note the very large value of C_p at the N - $Sm-A$ transition.

least-squares analysis of $\Delta C_p(T)/R$. The heating and cooling data clearly disagree near the C_p peak for the $X=0.40$ sample, indicating a coexistence region of about 50 mK. Similar differences between heating and cooling data near the C_p peak for the $X=0.50$ sample extended over 130 mK, indicating an even wider coexistence region. Comparison of the heating and cooling data for the $X=0.35$ sample indicates that if a coexistence region exists for this sample it must be narrower than 34 mK, and this range of data has been omitted from the subsequent analysis. The heating and cooling data disagree slightly in magnitude near the C_p peak for the $X=0.30$ sample,

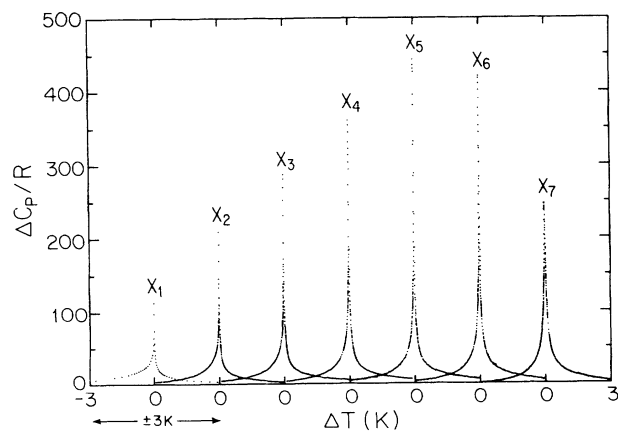


FIG. 5. Excess heat capacity $\Delta C_p/R$, in dimensionless units, associated with the N - $Sm-A$ transition in mixtures of 40.8+60.8. In each case, data are shown over the range $-3 \text{ K} < T - T_c < 3 \text{ K}$. The values of the mole fraction X of 60.8 are $X_1=0$ (pure 40.8), $X_2=0.10$, $X_3=0.20$, $X_4=0.30$, $X_5=0.35$, $X_6=0.40$, and $X_7=0.50$.

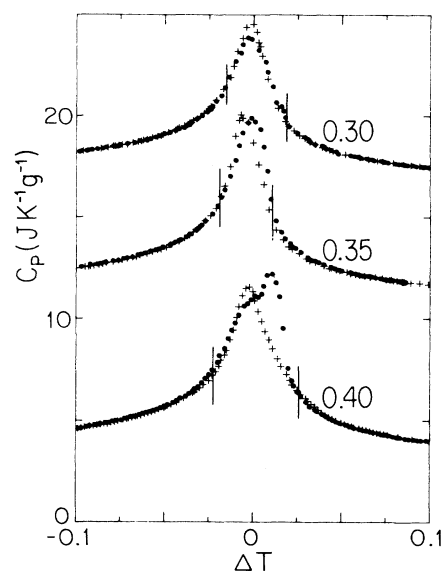


FIG. 6. A detailed comparison of heating (\bullet) and cooling (\circ) data near T_{NA} for mixtures with $X_{60.8}=0.30, 0.35$, and 0.40 . Typical scanning rates were 30 mK h^{-1} . $\Delta T = T - T_c$, where the T_c values are given in Table I. The data for the $X=0.35$ and $X=0.30$ samples have been shifted by $+7 \text{ J K}^{-1} \text{ g}^{-1}$ and $+14 \text{ J K}^{-1} \text{ g}^{-1}$, respectively. The vertical lines define the range of data points omitted from the least-squares fitting procedure.

and the peak is rounded over a 39-mK-wide region that has been omitted from the subsequent analysis. Similar rounding of 24 and 31 mK and slight disagreements in cooling and heating peak heights were observed in the $X=0.10$ and $X=0.20$ samples. This small rounding of liquid-crystal transitions is generally attributed to impurities and is quite common. We believe that the tricritical composition lies between 0.30 and 0.35 and is closer to $X=0.35$ than to $X=0.30$, as discussed in Sec. III.

The DSC measurements were carried out using a Perkin-Elmer DSC-4C instrument. It is convenient to define the quantity $DH_{NA} = \Delta H_{NA} + \delta H_{NA}$, where ΔH_{NA} is the latent heat associated with a first-order discontinuity in the enthalpy, and δH_{NA} is the pretransitional fluctuation contribution. The DSC and ac calorimetric data have been combined to obtain the values for DH_{NA} , ΔH_{NA} , and δH_{NA} as functions of $X_{60.8}$. The resulting values are presented in Fig. 7. The total enthalpy change across the N - $Sm-A$ transition is seen to increase monotonically with $X_{60.8}$. The latent heat ΔH_{NA} varies nonlinearly with $X_{60.8}$; it varies rapidly near pure 60.8 and goes to zero slowly at the tricritical point near $X_{60.8}=0.35$. The pretransitional (fluctuation) contribution $\delta H_{NA} = \int \Delta C_p dT$ reaches a maximum in the vicinity of the tricritical composition and decreases for larger or smaller concentrations of 60.8.

III. DATA ANALYSIS

The initial analysis of $\Delta C_p/R$ data has been carried out using the usual renormalization-group form

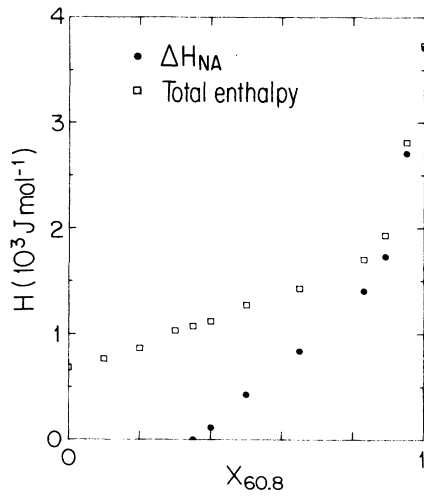


FIG. 7. Variation with composition of the latent heat ΔH_{NA} (●) and the total N -Sm- A enthalpy (□) $DH_{NA} = \Delta H_{NA} + \delta H_{NA}$. Note that the integrated fluctuation enthalpy $\delta H_{NA} = \int \Delta C_p dT$ is given by $DH_{NA} - \Delta H_{NA}$.

$$\frac{\Delta C_p}{R} = A^\pm |t|^{-\alpha} (1 + D_1^\pm |t|^{\Delta_1}) + B_c, \quad (4)$$

where $t \equiv (T - T_c)/T_c$ is the reduced temperature and the \pm superscripts denote above and below T_c . The coefficients D_1^\pm are the amplitudes of the first corrections-to-scaling terms, and Δ_1 has been taken to be $\frac{1}{2}$.⁴ The temperature-independent constant B_c is the critical contribution to the regular C_p variation.¹⁸ The results of fits using Eq. (4) over the range $|t| \leq 3 \times 10^{-3}$ are presented in Table I. It should be noted that the parameter values are cited with more digits than are justified by their standard deviations as obtained from the least-squares-fitting procedure. Although not all these digits

are “significant” in terms of describing the accuracy of a given parameter value, they are useful for generating the fitting curve over a large $\Delta C_p/R$ range without appreciable roundoff errors.

The fits described in Table I represent the $\Delta C_p/R$ data well, as indicated by the χ_v^2 values; and the results for the $X_{60.8} = 0.20$ sample are shown in Fig. 8 as an example. The effective α values exhibit an obvious trend with composition. An important aspect of these fitting results is the evolution in the role played by the correction amplitudes D_1^\pm . For the $X = 0.30, 0.35,$ and 0.40 samples, which are near the tricritical composition, the effect of the $(AD_1)^\pm |t|^{\Delta_1 - \alpha}$ terms is to introduce a rounded step-like C_p variation at T_c . If α and Δ_1 were exactly $\frac{1}{2}$, these terms would, indeed produce a discontinuous step ($A^+ D_1^+ - A^- D_1^-$) at T_c . It should be noted that the D_1^+, D_1^- , and B_c values are strongly coupled and highly uncertain when the α value is close to $\frac{1}{2}$. As an example, it can be shown that an equally good fit to the $X = 0.35$ data over the $|t| \leq 3 \times 10^{-3}$ range can be obtained with D_1^-/D_1^+ fixed at the theoretically expected value of unity.^{19,20} Such a fit yields $\alpha = 0.480$, $A^+ = 1.431$, $A^-/A^+ = 1.681$, $D_1^+ = -16.85$, $B_c = 14.5$, and $T_c = 345.826$ K with $\chi_v^2 = 1.52$. Thus, when α is close to $\frac{1}{2}$ and Δ_1 is taken as $\frac{1}{2}$, D_1^-/D_1^+ can be fixed at 1 and the fit merely adjusts the value of D_1^\pm to obtain the desirable steplike correction. This is not the case when α is different from $\frac{1}{2}$. Fixing $D_1^-/D_1^+ = 1$ for a fit to the $X = 0.20$ data yielded $\chi_v^2 = 1.96$, twice the value in Table I. It should be kept in mind that the unusual systematic trends in D_1^+, D_1^- , and B_c parameter values shown in Table I are an artificial effect of using Eq. (4) to mimic the complex crossover from second-order to tricritical behavior.

As pointed out above and discussed further below, steplike correction terms seem to arise naturally in fits to the $\Delta C_p/R$ data near the tricritical point in 40.8+60.8.

TABLE I. Results of fits to the $\Delta C_p/R$ data for 40.8+60.8 mixtures using Eq. (4) over the range $|t| \leq 3 \times 10^{-3}$. N is the number of data points included in these fits. Standard deviations are given for each least-squares parameter value except T_c , for which a standard deviation of ± 0.0002 K was obtained in all fits. The range of α values obtained by fitting this t range and the ranges $|t| \leq 10^{-3}$ and $|t| \leq 10^{-2}$ is given as $\Delta\alpha$.

$X_{60.8}$	N	α	A^+	A^-/A^+	D_1^+	D_1^-	B_c	T_c (K)	χ_v^2	$\Delta\alpha$
0	36 ^a	0.134	33.96	1.132	2.96	2.17	-78.3	336.877	1.10	0.123–0.152
		± 0.015	± 8.9	± 0.16	± 0.15	± 0.09	± 15			
0.10	121	0.222	15.50	1.284	6.90	3.41	-67.2	339.549	1.57	0.222–0.243
		± 0.012	± 2.8	± 0.018	± 0.32	± 0.27	± 8.9			
0.20	184	0.305	7.340	1.384	10.89	3.89	-56.2	342.707	0.98	0.305–0.320
		± 0.006	± 0.65	± 0.013	± 0.45	± 0.36	± 4.4			
0.30	154	0.456	1.723	1.621	10.82	0.82	-24.1	344.226	1.71	0.456–0.471
		± 0.014	± 0.23	± 0.032	± 11	± 6.3	± 17			
0.35	153	0.473	1.563	1.660	5.73	-3.29	-15.7	345.826	1.50	0.473–0.486
		± 0.012	± 0.21	± 0.035	± 24	± 29	± 34			
0.40	180	0.524	1.104	1.675	1.89	-6.66	-8.2	346.642	1.42	0.524–0.540
		± 0.013	± 0.18	0.046	± 34	± 140	± 42			

^aThese earlier 40.8 data were obtained using a manually operated calorimeter where data points were obtained at a series of fixed temperatures with fewer data points taken away from T_c .

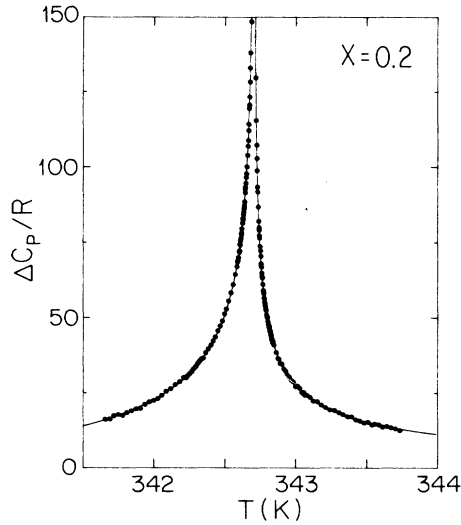


FIG. 8. Fit with Eq. (4) to $\Delta C_p/R$ for the 40.8+60.8 mixture with $X_{60.8} = 0.20$. The parameter values are given in Table I.

Such steps have also been reported for C_p at the tricritical point in other nonpolar systems: 6010+6012 mixtures¹¹ and 10S5, which is nearly tricritical.¹⁰ However, a step in C_p does not occur for tricritical N -Sm- A transitions in polar nCB mixtures.^{3,9} These facts are consistent with $(A^+D_1^+ - A^-D_1^-)$ as the source of the step. It is reasonable to expect that $D_1^+ \simeq D_1^-$ near a tricritical point in agreement with second-order behavior,^{19,20} but the tricritical amplitude ratio A^-/A^+ is not universal (see Sec. IV). For 40.8+60.8 and other nonpolar tricritical systems $A^-/A^+ \simeq 1.6$,^{10,11} which would create a step $(A^+D_1^+ - A^-D_1^-) \simeq -0.6A^+D_1^- > 0$ since D_1 is typically negative.²¹ For nCB mixtures $A^-/A^+ = 1.00$,^{3,9} and thus $(A^+D_1^+ - A^-D_1^-) \simeq 0$.

The value of Δ_1 is not well established at a tricritical point. If Δ_1 were significantly different from $\frac{1}{2}$, the $AD_1|t|^{\Delta-\alpha}$ correction terms could not generate a step at T_c for a tricritical sample. There is, however, another possible argument in support of a tricritical step. The inclusion of the eighth-order term in the classical Landau treatment of tricriticality will give (to a first approximation) a constant negative contribution to C_p for $T < T_c$. Thus this extended Landau treatment yields a step in the "background" in addition to the leading term that diverges like $\Delta T^{-1/2}$ below T_c .

Tricritical fits. We now wish to focus on a more detailed analysis of near-tricritical data. On the basis of the magnitude of the ΔC_p peaks and the effective α values discussed above, together with information presented in Sec. II, we believe that X_t is close to 0.35. All of the remaining analysis is carried out on the data for the sample with $X = 0.35$. This analysis is based on a more general form for $\Delta C_p/R$, which contains the first analytic correction terms $D_3^\pm t$ as well as higher-order nonanalytic corrections-to-scaling terms,²²

$$\frac{\Delta C_p}{R} = A^\pm |t|^{-\alpha} (1 + D_1^\pm |t|^{\Delta_1} + D_2^\pm |t|^{2\Delta_1} + D_3^\pm t + D_4^\pm t |t|^{\Delta_1}) + B. \quad (5)$$

In the absence of any clear indication to the contrary, we have adopted the value $\frac{1}{2}$ for Δ_1 at a tricritical point. As a result, the first corrections-to-scaling term merges with B and Eq. (5) becomes

$$\frac{\Delta C_p}{R} = A^\pm |t|^{-\alpha} (1 + D_2^\pm |t| + D_3^\pm t + D_4^\pm t |t|^{1/2}) + B^\pm, \quad (6)$$

where $\Delta B \equiv B^+ - B^- \neq 0$ due to $(A^+D_1^+ - A^-D_1^-) \neq 0$ and/or the role of the eighth-order terms in the free-energy functional. Equation (6) can be trivially simplified to

$$\frac{\Delta C_p}{R} = A^\pm |t|^{-\alpha} (1 + D_{23}^\pm |t| + \bar{D}_4^\pm |t|^{3/2}) + B^\pm, \quad (7)$$

where $D_{23}^+ = D_2^+ + D_3^+$ and $D_{23}^- = D_2^- - D_3^-$, $\bar{D}_4^+ = D_4^+$ and $\bar{D}_4^- = -D_4^-$.

The stability of fits with Eq. (7) on shrinking the range of reduced temperatures has been tested. Three ranges were used: range A ($|t| \leq 10^{-3}$), range B ($|t| \leq 3 \times 10^{-3}$), and range C ($|t| \leq 10^{-2}$). For fits of type 1 and 2, α was allowed to be a freely adjustable parameter and only one asymmetric correction terms was retained: $B^+ \neq B^-$ in type 1, and $D_{23}^+ \neq D_{23}^-$ with $B^+ = B^- = B$ in type 2. Table II gives the range dependence of two significant fitting parameters. The motivation for type-2 fits was the possibility that Δ_1 , the first corrections-to-scaling exponent, is not $\frac{1}{2}$ near a tricritical point but a larger value such as 1. There do not seem to be any theoretical predictions concerning this point. It is clear from Table II that type-2 fits are inferior to type-1 fits. However, both types showed a systematic pattern of deviations especially at larger $|t|$ values, which suggested the need for additional correction terms.

The remaining range-shrink tests were carried out on fits with α fixed at $\frac{1}{2}$, which seems justified in view of free α values that lie in the range 0.473–0.510.²³ Three fitting variants (types 3, 4, and 5) are summarized in Table II. In type-3 fits, both a step in B and correction terms linear in t are allowed. The constraint $B^+ = B^-$ is imposed in type-4 fits, but the number of adjustable parameters is the same as for type 3. The type-5 fit is the most general form and yields a significantly (at the 95% confidence level) lower χ^2_ν value for range C .

The complete set of parameter values for fits 1, 4, and 5, as obtained from fitting range C , is given in Table III. These three fits represent the statistically and physically most attractive possibilities. The $\Delta C_p/R$ data and the theoretical curve for fit 1 are shown over range C in Fig. 9. Although the overall quality of this fit is quite good, systematic deviations are obvious on the residuals plot shown in Fig. 10. The residuals obtained from fit 5 are much smaller, as shown in Fig. 11, but the pattern of deviations is still not completely random for $T < T_c$. A

TABLE II. Partial results of five different types of fit with Eq. (7) to the $X_{60.8}=0.35$ data over three ranges of reduced temperature. The minimum reduced temperatures for $T > T_c$ and $T < T_c$ are $t_{\min}^+ = 3.8 \times 10^{-5}$ and $|t_{\min}^-| = 6.1 \times 10^{-5}$ in every case, but t_{\max} is varied. The constraints are as follows: type 1, $D_{23}^\pm = \bar{D}_4^\pm = 0$; type 2, $\Delta B = B^+ - B^- = 0$ and $\bar{D}_4^\pm = 0$; type 3, $\alpha = \frac{1}{2}$ and $\bar{D}_4^\pm = 0$; type 4, $\alpha = \frac{1}{2}$ and $\Delta B = B^+ - B^- = 0$; type 5, $\alpha = \frac{1}{2}$. Values in parentheses are held fixed at the specified values. χ_v^2 values are given in square brackets.

Range	α free				$\alpha = \frac{1}{2}$ fixed						
	Type 1 α	ΔB	Type 2 α	D_{23}^+	Type 3 ΔB	D_{23}^+	Type 4 D_{23}^+	\bar{D}_4^+	ΔB	Type 5 D_{23}^+	\bar{D}_4^+
<i>A</i> $ t \leq 10^{-3}$	0.477 [1.73]	13.3	0.495 [1.85]	5.0	(8.8) [1.77]	(-38)	(-55) [1.69]	(110)	(2.1) [1.69]	(-46)	(33)
<i>B</i> $ t \leq 3 \times 10^{-3}$	0.473 [1.52]	15.3	0.502 [1.78]	7.6	8.8 [1.60]	-38	-55 [1.48]	110	2.1 [1.46]	-46	33
<i>C</i> $ t \leq 10^{-2}$	0.484 [2.77]	12.0	0.510 [6.65]	13	16.3 [2.29]	-40	-42 [1.71]	86	7.7 [1.37]	-45	40

comparison of fit curve 5 with the data over range *A* ($|t| \leq 10^{-3}$) and a smaller range ($|t| \leq 3 \times 10^{-4}$) is given in Fig. 12. It should be stressed that no additional adjustment of the parameters has been made to improve the fit over these inner ranges. The curves in Fig. 12 are obtained using parameters from the fit over range *C*. Note that several omitted points on both sides of T_c actually fit curve 5 quite well; their inclusion in the data set would not alter the values of the adjustable parameters in Eq. (7).

It is well known that logarithmic corrections are expected at tricritical points since the upper marginal dimension d_u is 3. We have fit the $X=0.35$ data using two forms for the logarithmically corrected heat capacity at a tricritical point. Using the scaling form given by Lawrie and Sarbach¹⁵ for the singular free energy, one obtains the following result for the asymptotic heat capacity variation:

$$\frac{\Delta C_p}{R} = A^\pm |t|^{-1/2} (1 + L^\pm \ln|t|)^q + B_c, \quad (8)$$

where $q = -6(n+4)/(3n+22) = -\frac{9}{7}$ for an *XY* model ($n=2$). If L^- is set equal to zero, then the effective amplitude ratio defined as

$$\left(\frac{A^-}{A^+} \right)_{\text{eff}} = \frac{A^-}{A^+} (1 + L^+ \ln|t|)^{-q} \quad (9)$$

will asymptotically approach the classical limit of $A^-/A^+ = \infty$ (i.e., $A^+ = 0$) in agreement with the general predictions of Stephen²⁴ (see Sec. IV). If $L^+ = L^-$ and $B_c^+ = B_c^-$ is required for fits with Eq. (8), no improvement over fits using a simple power law²³ is achieved and the L^\pm values are close to zero. If L^- is set to zero then fits of moderate quality are obtained with $\chi_v^2 = 1.90$ for range *A*, 2.41 for range *B*, and 3.16 for range *C*. These fits are not as good as those given in Table II. For the fit to range *C* one obtains $A^+ = 6.97$, $A^-/A^+ = 0.293$, $L^+ = -0.299$, $L^- = 0$, $B_c = -18.6$, and $T_c = 345.828$ K. The $(1 + L^+ \ln|t|)^q$ term can be viewed as a correction to the amplitude A^+ or as the source of the unusual effective background variation²⁵ shown in Fig. 9. We have also tried using the form predicted by Gorodetskii and Zaprudskii¹⁶ for the logarithmically corrected heat capacity at a tricritical point,

$$\frac{\Delta C_p}{R} = \frac{A^\pm}{b} |t|^{-1/2} \left[\ln \frac{b^2}{|t|} \right]^{\mp 0.5} + B_c, \quad (10)$$

TABLE III. Least-squares parameter values (with their standard deviations) for fitting $\Delta C_p/R$ data on the near-tricritical 40.8+60.8 mixture with $X=0.35$. These fits were made with Eq. (7) over range *C* ($|t| \leq 10^{-2}$) and correspond to fits of type 1, 4, and 5 from Table II. Values in parentheses were held fixed at the given value. T_c was a freely adjustable parameter and had the value 345.826 K for all three fits. A χ_v^2 value is given for range *A* ($|t| \leq 10^{-3}$) and range *B* ($|t| \leq 3 \times 10^{-3}$) as well as range *C*; no further adjustment of parameters was made in evaluating the χ_v^2 values for ranges *A* and *B*.

Fit	α	A^+	A^-/A^+	B^+	B^-	D_{23}^+	D_{23}^-/D_{23}^+	\bar{D}_4^+	\bar{D}_4^-/\bar{D}_4^+	$\chi_v^2(C)$	$\chi_v^2(B)$	$\chi_v^2(A)$
1	0.484 ± 0.002	1.402 ± 0.028	1.633 ± 0.008	-7.6 ± 0.2	-19.7 ± 0.4	(0)	(1)	(0)	(1)	2.77	2.32	1.91
4	(0.5)	1.174 ± 0.006	1.578 ± 0.004	-2.9 ± 0.6	-2.9 ± 0.6	-42 ± 13	5.0 ± 1.4	86 ± 90	17 ± 25	1.71	1.78	1.96
5	(0.5)	1.163 ± 0.007	1.651 ± 0.011	-2.1 ± 0.7	-9.8 ± 2.9	-45 ± 15	2.6 ± 1.0	40 ± 110	22 ± 70	1.37	1.54	1.84

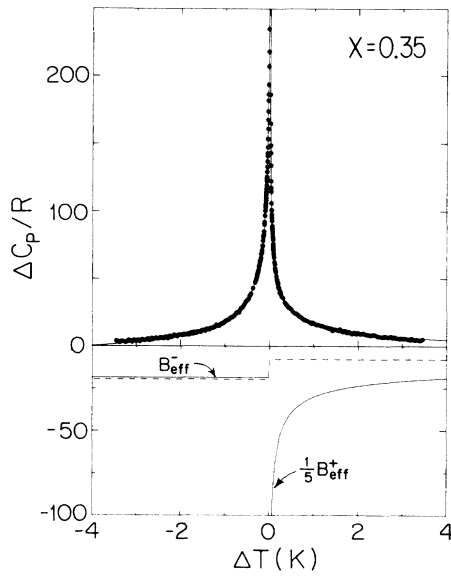


FIG. 9. Fit with Eq. (7) to the tricritical $\Delta C_p/R$ data for the 40.8+60.8 mixture with $X_{60.8}=0.35$. The range of the fit is $|t| \leq 10^{-2}$. The critical exponent α is 0.484; other parameter values are given under fit 1 in Table III. The dashed line represents the background term B^\pm , which has a step at T_c . The continuous curve in the lower box represents the “effective” background B_{eff}^\pm associated with the logarithmic-correction form given by Eq. (8); see footnote 25. Note that the vertical scale is slightly expanded in the lower box.

where a second logarithmic correction term $1.579(\ln b^2/|t|)^{-0.5}$ occurring for $T < T_c$ has been ignored since it is numerically much smaller than $(\ln b^2/|t|)^{+0.5}$ for our system. Gorodetskii and Zaprudskii explicitly

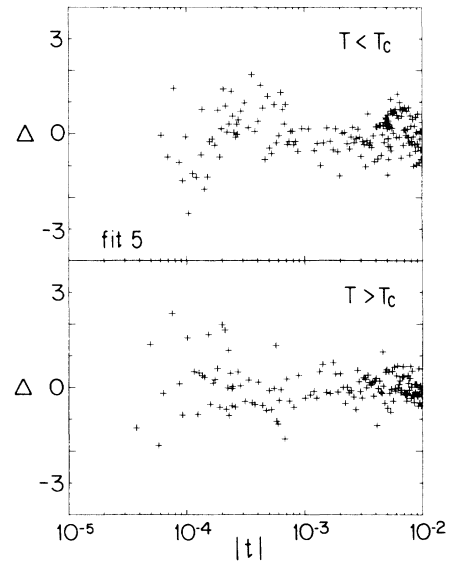


FIG. 11. Deviations $\Delta \equiv \Delta C_p/R(\text{obs}) - \Delta C_p/R(\text{fit})$ for fit 5 in Table III.

predict that $A^-/A^+ = 3.56$. This form cannot provide even a qualitatively acceptable fit to the data for the $X=0.35$ sample since the experimental peak is close to symmetric ($A^-/A^+ \approx 1.6$) while the equations given in Ref. 16 predict almost no excess heat capacity for $T > T_c$. In particular, Eq. (10) yields the effective amplitude ratio

$$\left[\frac{A^-}{A^+} \right]_{\text{eff}} = \frac{A^-}{A^+} (\ln b^2 - \ln |t|). \tag{11}$$

Since the value of b^2 from (very poor) least-squares fits

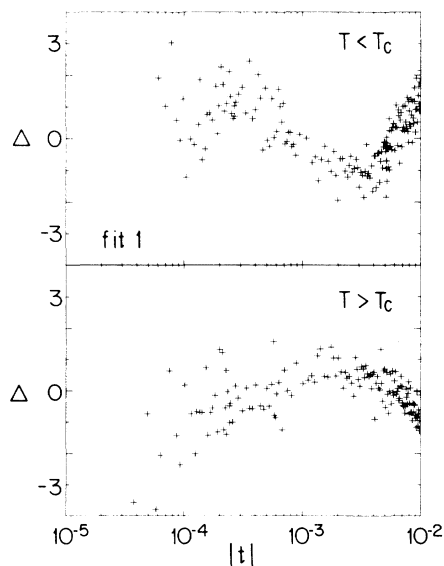


FIG. 10. Deviations $\Delta \equiv \Delta C_p/R(\text{obs}) - \Delta C_p/R(\text{fit})$ for fit 1 in Table III.

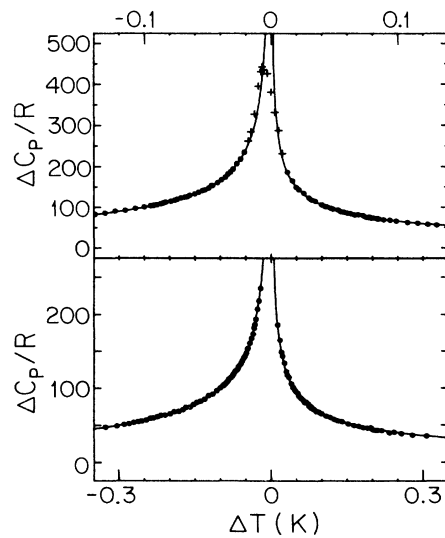


FIG. 12. Fit 5 to the tricritical $\Delta C_p/R$ data over range A ($|t| \leq 10^{-3}$) and the range $|t| \leq 3 \times 10^{-4}$. Data points omitted from the fitting procedure are shown here as plus signs.

with Eq. (10) is 18.3, Eq. (11) predicts that $(A^-/A^+)_{\text{eff}}$ should vary from 27 at $|t|=10^{-2}$ to 43 at $|t|=10^{-4}$, which is clearly inconsistent with our data.

IV. DISCUSSION

The effective N -Sm- A critical exponent α for mixtures of the homologous compounds 40.8 and 60.8 increases with $X_{60.8}$ from $\alpha=0.13$ for pure 40.8 to $\alpha \simeq 0.50$ for the near-tricritical mixture with $X=0.35$. It is thought that this represents crossover behavior between 3D- XY second-order behavior and tricritical behavior. However, the general validity of the XY model for N -Sm- A transitions in nonpolar systems is not well established,^{2,3} and no quantitative crossover form for C_p exists. As shown in Fig. 5, the magnitude of the N -Sm- A excess heat capacity increases monotonically from 40.8 up to the tricritical composition and then decreases as X increases further. This occurs because the Sm- A fluctuations become stronger as the nematic range decreases. When the transition becomes first order, part of the enthalpy change becomes a discontinuous latent heat and the pretransitional integrated enthalpy decreases.^{3,9,11} In terms of two-scale-factor universality the increase in the amplitude of the heat capacity can be related to decreases in the magnitude of the bare correlation lengths as the nematic range decreases.³

For the near tricritical sample with $X=0.35$, the exponent α is very close to the expected Gaussian tricritical value of $\frac{1}{2}$. Indeed, the data are fully consistent with $\alpha=0.50$ when correction terms are taken into account. There is, however, the possibility that α is slightly less than 0.50 for this sample (see fit 1 in Table III). It does not seem likely that this is due to the composition being different from the exact tricritical value X_t . Figure 6 suggests that $X=0.35$ may be slightly larger than X_t , and one would thus expect $\alpha_{\text{eff}} > 0.5$. A possible explanation for an exponent value less than $\frac{1}{2}$ can be given in terms of incipient Fisher renormalization.²⁶ It is well known that C_p values measured along a constant composition path should asymptotically exhibit the renormalized exponent $\alpha_R = -\alpha/(1-\alpha)$,²⁶ which equals -1 for a tricritical system. The extent of such renormalization depends on the magnitude of $(dT_c/dX)^2$ among other factors. The observation of an effective α value of 0.48 for C_{pX} at a tricritical point could thus be explained as due to the early stages of crossover from $\alpha=\frac{1}{2}$ to $\alpha_R=-1$ as $|t| \rightarrow 0$. Complete renormalization has been observed in systems with $dT_{NA}/dX \geq 230$ K,^{12,27} and no evidence of renormalization is observed when $(dT_{NA}/dX) \leq 10.8$ K (see Table III in Ref. 12). For a 40.8+60.8 mixture with $X=0.35$, $dT_{NA}/dX=19.3$ K, which might be large enough to cause incipient crossover. Although we cannot rule out this possibility, it seems more likely that fit 1 yields $\alpha=0.48$ due to the neglect of important correction terms.

The tricritical amplitude ratio $A^-/A^+ \simeq 1.6$ for 40.8+60.8 is similar to those observed in other nonpolar mixtures^{10,11} but differs from the value 1.0 observed in polar cyanobiphenyls.^{3,9} This is not an issue of concern

since it is known that tricritical A^-/A^+ ratios determined over accessible $|t|$ ranges are not universal. Fisher and Sarbach²⁸ showed that the amplitude ratios at the tricritical point in an exactly solvable spherical ($n=\infty$) model were nonuniversal but functions of the single variable $z=(a/R_0)^3$, where a is the lattice spacing and R_0 specifies the range of interaction. This theory was successful in explaining the experimentally available ratios for ^3He - ^4He mixtures and for the metamagnet $\text{Dy}_3\text{Al}_5\text{O}_{12}$ [dysprosium aluminum garnet (DAG)] with $z=0.12$ and $z=0.21$, respectively. The amplitude ratios predicted by Landau theory are recovered for $z=0$. Stephen²⁴ has pointed out the relation between the apparent nonuniversality of amplitude ratios and the logarithmic correction factor expected for real systems with $d=3$ and finite n . It is predicted that the presence of the logarithmic terms will slowly drive z to zero as $|t| \rightarrow 0$ and restore the amplitude ratios to the Landau-theory values. The approximation of taking z to be a constant will work well if the logarithmic corrections are small. Using the results of Fisher and Sarbach,²⁸ we find $A^-/A^+ = (1-z^2)^{1/2}/z$, which yields $z=0.530$ for $A^-/A^+=1.6$ and $z=0.707$ for $A^-/A^+=1.0$. The fact that the inclusion of logarithmic correction terms in Eq. (8) did not yield an improved fit to the tricritical 40.8+60.8 data shows that logarithmic corrections do not play a dominant role. Thus the constant- z approximation should work well for the N -Sm- A tricritical point. Values of z such as 0.53 and 0.71 show that N -Sm- A tricriticality is further from the classical Landau result (for which $z=0$) than the tricritical behavior in ^3He - ^4He mixtures or DAG.

The fitting results given in Tables II and III suggest that higher-order correction terms may play an important role for the tricritical 40.8+60.8 mixture, especially over a range as wide as $|t| \leq 10^{-2}$. It is seen from Table III that the D_{23}^-/D_{23}^+ ratio is greater than 1, perhaps even as large as 5. This is not necessarily inconsistent with the general expectation that correction amplitude ratios should be close to unity.¹⁹ Since both analytic and non-analytic terms contribute to this correction term, $D_{23}^-/D_{23}^+ = (D_2^- - D_3^-)/(D_2^+ + D_3^+)$. Thus, negative $D_2^+ \simeq D_2^-$ values and positive $D_3^+ \simeq D_3^-$ values with $|D_2| > D_3$ could lead to the observed negative D_{23}^\pm values with a ratio $D_{23}^-/D_{23}^+ > 1$. The \bar{D}_4^\pm values are very uncertain and suspiciously large, especially \bar{D}_4^- . Unfortunately, there is a strong coupling between $\Delta B = B^+ - B^-$, D_{23}^\pm , and \bar{D}_4^\pm . For fits 4 and 5, the $A^\pm D_{23}^\pm |t|^{1/2}$ terms play a significant role even over range A ($|t| < 10^{-3}$). Since $D_{23}^-/D_{23}^+ > 1$ and both D_{23}^+ and D_{23}^- are negative, these correction terms have an effect over range A that is crudely analogous to a positive step ΔB . Large positive \bar{D}_4^\pm values are then required to offset the negative contributions of $A^\pm D_{23}^\pm |t|^{1/2}$ over wider reduced temperature ranges. Although the present data do not resolve the relative importance of several possible correction terms, there is strong evidence for a steplike $\Delta C_p/R$ variation at T_c . It would be of interest to carry out a high-resolution x-ray study of 40.8+60.8 to determine the critical exponents γ , ν_{\parallel} , and ν_{\perp} and to look for the possible appearance of correction terms in the behavior of the suscepti-

bility and the correlation lengths.

In summary, the effective critical exponent α evolves monotonically with the 60.8 mole fraction X in 40.8+60.8 mixtures. For the near-tricritical sample with $X=0.35$, the C_p data are consistent with the tricritical value $\alpha=0.5$. The nonuniversal tricritical amplitude ratio $A^-/A^+=1.6$ can be understood in terms of the Sarbach-Fisher model.²⁸ Steplike correction terms seem to be required for fitting data near the tricritical point. A step discontinuity at T_c would arise naturally as a consequence of $A^-/A^+\neq 1$ if the first corrections-to-scaling exponent Δ_1 is $\frac{1}{2}$ at a tricritical point.

ACKNOWLEDGMENTS

We wish to thank P. Leach for performing the DSC measurements and Dr. M. Meichle for the ac calorimeter results on 60.8. We also thank Dr. M. Neubert of the Liquid Crystal Institute at Kent State University for supplying the liquid-crystal materials. We greatly appreciate helpful discussions with A. Aharony, M. E. Fisher, M. J. Stephen, and J. Thoen. This work was supported by National Science Foundation (NSF) Grant No. DMR-87-19217.

- ¹J. Prost, *Adv. Phys.* **33**, 1 (1984); T. C. Lubensky, *J. Chim. Phys.* **80**, 31 (1983).
- ²C. W. Garland, M. Meichle, B. M. Ocko, A. R. Kortan, C. R. Safinya, L. J. Yu, J. D. Litster, and R. J. Birgeneau, *Phys. Rev. A* **27**, 3234 (1983), and references cited therein.
- ³J. Thoen, H. Marynissen, and W. van Dael, *Phys. Rev. Lett.* **52**, 204 (1984); B. M. Ocko, R. J. Birgeneau, and J. D. Litster, *Z. Phys. B* **62**, 487 (1986).
- ⁴J. C. LeGuillon and J. Zinn-Justin, *Phys. Rev. Lett.* **39**, 95 (1977); *Phys. Rev. B* **21**, 3976 (1980).
- ⁵C. A. Schantz and D. L. Johnson, *Phys. Rev. A* **17**, 1504 (1978).
- ⁶J. Thoen, H. Marynissen, and W. van Dael, *Phys. Rev. A* **26**, 2886 (1982).
- ⁷R. J. Birgeneau, C. W. Garland, G. B. Kasting, and B. M. Ocko, *Phys. Rev. A* **24**, 2624 (1980).
- ⁸G. B. Kasting, K. J. Lushington, and C. W. Garland, *Phys. Rev. B* **22**, 321 (1980).
- ⁹H. Marynissen, J. Thoen, and W. van Dael, *Mol. Cryst. Liq. Cryst.* **124**, 195 (1985).
- ¹⁰D. Brisbin, R. DeHoff, T. E. Lockhart, and D. L. Johnson, *Phys. Rev. Lett.* **43**, 1171 (1979); D. J. Johnson (private communication).
- ¹¹M. A. Anisimov, V. P. Voronov, A. O. Kulkov, V. N. Petukhov, and F. Kholmurodov, *Mol. Cryst. Liq. Cryst.* **150**, 399 (1987).
- ¹²M. E. Huster, K. J. Stine, and C. W. Garland, *Phys. Rev. A* **36**, 2364 (1987).
- ¹³E. K. Riedel and F. J. Wegner, *Phys. Rev. B* **9**, 294 (1974).
- ¹⁴M. Meichle (private communication). An attempt to induce a change to second-order behavior for the N -Sm- A transition of pure 60.8 by applying pressure, which broadens the nematic range, failed because the Sm- A phase disappeared at a Sm- A -Cr- B - N triple point before the N -Sm- A transition became second order.
- ¹⁵I. D. Lawrie and S. Sarbach, in *Phase Transitions and Critical Phenomena*, edited by C. Domb and J. L. Lebowitz (Academic, New York, 1984), Vol. 9, p. 124; M. J. Stephen, E. Aharony, and J. P. Straley, *Phys. Rev. B* **12**, 256 (1975).
- ¹⁶E. E. Gorodetskii and V. M. Zaprudskii, *Zh. Eksp. Teor. Fiz.* **39**, 2299 (1977) [*Sov. Phys.-JETP* **45**, 1209 (1977)].
- ¹⁷C. W. Garland, *Thermochim. Acta* **88**, 127 (1985).
- ¹⁸C. Bagnuls and C. Bervillier, *Phys. Lett.* **107A**, 299 (1985).
- ¹⁹A. Aharony and G. Ahlers, *Phys. Rev. Lett.* **44**, 782 (1980).
- ²⁰M. C. Chang and A. Houghton, *Phys. Rev. B* **21**, 1881 (1980).
- ²¹C. W. Garland, G. Nounesis, and K. J. Stine (unpublished).
- ²²A. Aharony and M. E. Fisher, *Phys. Rev. B* **27**, 4394 (1983); A. Aharony (private communication).
- ²³The fits of Eq. (7) to $X=0.35$ data with $B^-=B^+$ and $D_{23}^+=\bar{D}_4^\pm=0$ are poorer than the fits of type 1 and type 2 in Table II but still give α close to $\frac{1}{2}$. The critical exponents were $\alpha=0.498$ for range A ($\chi_v^2=5.7$), 0.499 for range B ($\chi_v^2=20$), and 0.499 for range C ($\chi_v^2=32$).
- ²⁴M. J. Stephen, *J. Phys. C* **13**, L83 (1980).
- ²⁵The variation shown in Fig. 9, which represents an effective background B_{eff}^\pm for Eq. (8) is obtained from $B_{\text{eff}}^-=B_c$ and $B_{\text{eff}}^+=B_c+A^+|t|^{-1/2}(1+L^+|\ln|t||)^q-A^+|t|^{-1/2}$.
- ²⁶M. E. Fisher, *Phys. Rev.* **176**, 257 (1968); P. E. Scesney and M. E. Fisher, *Phys. Rev. A* **2**, 825 (1970); see also Ref. 12.
- ²⁷K. J. Stine and C. W. Garland, *Phys. Rev. A* **39**, 1482 (1989).
- ²⁸M. E. Fisher and S. Sarbach, *Phys. Rev. Lett.* **41**, 1127 (1978); S. Sarbach and M. E. Fisher, *Phys. Rev. B* **20**, 2797 (1979).